Proceedings of ISFA2016
2016 International Symposium on Flexible Automation
Cleveland, Ohio, U.S.A., 1 - 3 August, 2016

ADAPTIVE SYNCHRONIZATION OF NETWORKED MULTI-AGENT SYSTEMS CONSIDERING TRANSIENT RESPONSES AND DISTURBANCES

Theophilus Okore-Hanson
Department of Mechanical Engineering,
North Carolina A&T State University
1601 East Market Street
Greensboro, NC, 27411
tokoreha@aggies.ncat.edu

Sun Yi
Department of Mechanical Engineering,
North Carolina A&T State University
1601 East Market Street
Greensboro, NC, 27411
syi@ncat.edu

ABSTRACT
Networks of mechanical drive systems require precise and robust regulation of the position and speed relations at specified synchronized ratios. Successful synchronization of the multi-agent systems can provide complex mechanisms like powertrain drives or precision machines with enhanced efficient and effective performances. In this paper a new adaptive tracking and synchronization controller is presented to achieve robust tracking and synchronization performance under modeling errors and disturbances. The presented methodology combines a synchronization method of networked systems and model reference adaptive control theories considering uncertainties. Improved transient and steady-state system performances are validated through application of the proposed architecture to DC servo motor systems.

1.0 INTRODUCTION
Synchronization of multi-agent systems is an important task in control of robotic arms, electric trains, numerical control machines, hydraulic lifts, plotters, tele-surgery, etc. Motion synchronization of networked systems is challenging due to uncertainties and has attracted a lot of research interests. Traditional synchronization of multi-agent systems has been achieved by mechanical hard coupling of a central motion source using shafts, gears, belts, etc. These mechanisms determine the speed and position relationship among the various motion axes. Driveline losses and wear of machine parts over a short cycle of machine run may create critical problems and huge losses for manufacturing industries due to reduced accuracy. With application of closed-loop multi-agent synchronization approach, the aforementioned drawbacks in the mechanical synchronization technics can be resolved. Multi-agent synchronization provides numerous advantages over traditional synchronization methods. Some of the advantages associated with multi-agent synchronization mentioned in [1] are:

- Inherent capacity to maintain synchronization between drive axes during transient time and under load disturbances.
- Fast response to load changes, start-up, and shutdown conditions.
- A significant increment in the tighter machine stiffness (synchronization between components) than a mechanical shaft offers.
- Non-dissipative shaft damping
- Wide areas of application in diverse engineering fields

Multi-axes synchronization techniques are widely employed in manufacturing processes and applications where precise control of position, speed, acceleration and deceleration are required [2]. As solutions, it was shown in [3, 4] that the mechanical line shaft can be replaced by sectional drives and synchronized electronically.

Various techniques aimed at achieving multi-axes synchronization have been developed over the last decade. Synchronization can be achieved by either the “equal-status” approach or the “master-slave” approach [5]. In the equal-status approach, the synchronization controller treats multiple axes the same without favoring one axis over the others. Thus, when dynamics are significantly different among multiple axes, the equal status approach may not be a suitable option, because the synchronization speed of the overall system is set to the slowest axis [6]. In a two-axis problem with significantly different dynamics between the two axes, the master-slave approach is more favorable. In this case, the slow axis acts as the master for the fast axis. The fast axis, the slave, follows the slow axis the

978-1-5090-3466-6/16/$31.00 ©2016 IEEE

master. In the master-slave configuration, the output speed of the master serves as the speed reference for the slave. Consequently, any speed or load disturbances applied to the master is transferred to the slave, but that of any slave does not affect the master or any other slave. This layout is recommended for applications where synchronization in speed and position are not critical, because synchronization when disturbances exist is not guaranteed [7].

For better synchronization performance, cross-coupled control synchronization was proposed for generating predetermined path under load disturbances such as encountered in NC and CNC machine tools [7]. The control mechanism has an additional feedback signal, generated from the relative speed and angular differences between the two systems. The differences are fed back into the input of the controllers. The proportional plus derivative (PD) type controller with feedback of this coupled position error leads asymptotic convergence to zero of both position and synchronization errors for a set point motion control. However, this technique lacks the stiffness property inherent in hard mechanical coupled systems.

An approach to address the lack of stiffness property in the virtual synchronization is the Electronic Virtual Line Shafting configuration. This technique, however, lacks a position controller. There exists lack of position synchronization during start up, load disturbances and, in general, non-zero constant steady-state errors. For this reason, it has been applied to systems where speed differences is not critical [4].

For better synchronized speed responses in all motors during the initial transient period and load torque variation, the Relative Coupling Strategy was introduced [8]. This scheme is based on the Cross Coupling Control, (a.k.a Equal Status Control). It has a speed relative command between the motors, which is added to the velocity signal as damping coefficient of each motor system. This arrangement is not based on the general master reference used in the Electronic Virtual Line shafting. Therefore, the inertia of each motor is integrated into the relative speed block. The controller has a relative error signal. An additional advantage is the capability of application to more than two motors. The relative block sets the relative difference between motors to zero during transient and torque disturbance periods. In designing the relative feedback block, parameters necessary are moment of Inertia (J), friction related to each motor (b); natural frequency (ω_n) and damping coefficient (ζ) of the whole system [1].

This paper presents the adaptive tracking and synchronization performance of a multi-agent system with Relative Coupling scheme. Each individual system is designed with its' own controllers to guarantee a good tracking performance. Experiments are performed first with 2 agents, and then 3 agents with introduction of disturbance on one of the agents in both cases to ascertain efficacy of the proposed adaptive synchronization control scheme. The 3-agent multi-synchronization scheme is also used to validate the applicability of the proposed synchronization technic to n-agents. In [9], major concerns such as the transient performance and robustness under torque load disturbance were not considered. This paper looks at ways to improve tracking and synchronization under load torque disturbance and transient error reduction. In [5] the incorporation of a cross-coupled compensator to an adaptive feed-forward scheme was introduced to improve transient response and disturbance rejection properties. In [10-13] it was shown that the kinematic relationship in a multi-agent synchronization system can be formulated as guiding and positioning the agents along a boundary of compact set with cross-coupling feedback loops. Time varying formation was also proposed. In model reference adaptive control (MRAC) the output response of the plant is forced to track the reference model irrespective of plant parameter variations [14-16]. The difference in the output of the model and the plant, which is the error, is fed into the adjustment mechanism and the output from the adjustment mechanism is used to tune the controller such that the plant output behaves like the model. In this paper, the adaptive control is used for synchronization of DC servo-motors. Disturbance is introduced in one of the agents in the synchronization by eccentrically loading one of the motors. The system's response is compared for an over-damped and critically-damped reference model with/without a synchronizing controller. The reference model specifies the desired performance criteria. The controller is comprised of the adjustment parameters identified as β_1 and β_2 .These parameterizations are linear in nature. The values of these control parameters are mainly dependent on the adaptation gain, which affects the convergence speed. The adaptation mechanism is used to adjust the parameters in the controller to ensure that the plant's response asymptotically approaches the reference model. The MIT rule, Lyapunov theory, and augmented error theory can be used to develop the adaptation Mechanism. The MIT rule is used in this paper because it is widely used in similar applications.

2.0 SYSTEM SETUP

The experiment is performed with a Quanser Personality Intelligent Data acquisition (QPID) device, a PC, two amplifiers and Quanser SRV02 motors integrated with single ended optical shaft encoders offering a high resolution of 4096 counts per revolution. The QPID receives encoder signals from the motors, sends analog output signals to the power amplifier and receives analogue/digital signals from the power amplifier. The encoders read the angular positions of the motors and send to the DAQ. Analog sensor signals are read through the analog input channels of the DAQ and then outputted through the DAC connector of the acquisition device to the power amplifier. The amplifier then sends the amplified control voltage to the motors.

In order to evaluate performance of the adaptive synchronization controller, one of the motors is eccentrically loaded with a flying 100g weight, 10cm away from the center as displayed in Fig 2. In Fig 1, the system setup is shown without disturbance.

Figure 1: Two motor system; using angular motion sensors, state variables are collected

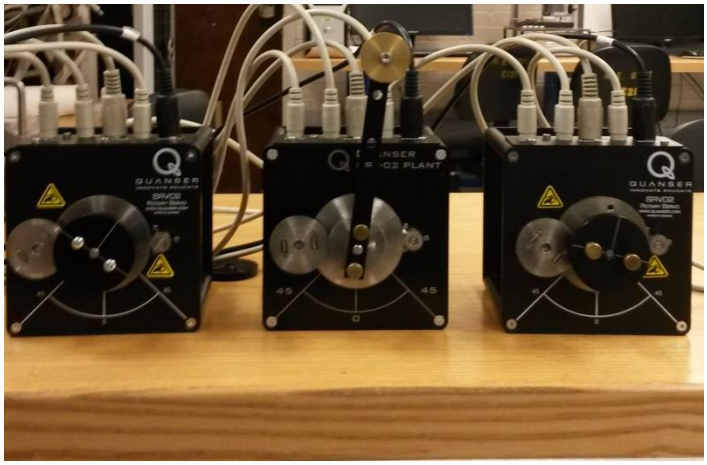

Figure 2: Setup of 3-agent system with disturbance; a flying mass is hanged to introduce disturbance

3.0 DC MOTOR MODELING

The dynamics of a DC motor with negligible armature inductance and load torque disturbance $T_{l(t)}$ can be represented by;

$$J_m\ddot{\theta}_m + b\dot{\theta}_m = K_t i_a + T_l \tag{3.1}$$

$$K_b\dot{\theta}_m + R_a i_a = v_a \tag{3.2}$$

Taking Laplace transform we have

$$J_m\theta_m s^2(s) + b\theta_m s(s) = K_t i_a(s) + T_l(s) \tag{3.3}$$

$$K_b\theta_m s(s) + R_a I_a(s) = V_a(s) \tag{3.4}$$

Solving for I_a in Eq.(3.4) and substituting in Eq.(3.3) the equation for the motor position becomes

$$\left(J_m R_a s^2(s) + bR_a s(s) + K_b s(s)\right)\theta_m =$$

$$K_t V_a(s) + R_a T_l(s) \tag{3.5}$$

$$\left(\frac{J_m R_a}{bR_a s(s) + K_t K_b s(s)} s^2 + 1\right)\theta_m(s) =$$

$$= \frac{K_t}{bR_a s(s) + K_t K_b s(s)} V_a(s) + \frac{R_a \quad T_l(s)}{bR_a s(s) + K_t K_b s(s)} \tag{3.6}$$

Simplifying the coefficients in equation (6) by defining new parameters as

$$(\tau s^2 + 1)\theta_m(s) = AV_a(s) + BT_l(s) \tag{3.7}$$

where,

$$\tau = \frac{J_m R_a}{bR_a s(s) + K_t K_b s(s)}$$
$$A = \frac{K_t}{bR_a s(s) + K_t K_b s(s)} \tag{3.8}$$
$$B = \frac{R_a}{bR_a s(s) + K_t K_b s(s)}$$

The transfer function of equation Eq. (7) can be written as

$$\theta_m(s) = \frac{A}{(\tau s^2 + 1)} V_a(s) + \frac{B}{(\tau s^2 + 1)} T_l(s) \tag{3.9}$$

The motor transfer function assuming load torque $T_l = 0$

$$\frac{\theta_m}{V_a} = \frac{K}{s(\tau s + s)} \tag{3.10}$$

4.0 MODEL REFERENCE ADAPTIVE CONTROLLER

In model reference adaptive control Figure 1, reference model is driven by a command signal u_c, the goal is to let the plant's output to be exactly same as the reference model. The difference between the reference model and the plant is the error. The error drives the update law and the update law tunes the controller such that the uncertain plant's output will behave like the reference model output.

The reference model is selected such that transient oscillation is reduced and system's performance is desired.
The reference model is selected as,

$$G_m(s) = \frac{a_{0m}}{s^2 + a_{1m}s + a_{0m}} \tag{4.1}$$

$$e = y_{plant} - y_{model} \tag{4.2}$$

A cost function J is selected such that the parameters are adjusted to minimize J.

$$J(\beta) = \frac{1}{2}e^2(\beta) \tag{4.3}$$

To make J small the parameters are changed in the direction of the negative gradient of J, that is; the error decays with time.

$$\frac{d\beta}{dt} = -\gamma \frac{\delta J}{\delta \beta} = -\gamma e \frac{\delta e}{\delta \beta} \tag{4.4}$$

$$u = \beta_1 u_c - \beta_2 y_{plant} = G_p u - G_m u_c \tag{4.5}$$

$$y_{plant} = G_p u = \frac{1.53}{0.0254s^2 + s}\left(\beta_1 u_c - \beta_2 y_{plant}\right) \tag{4.6}$$

$$y_{plant} = \frac{1.53\beta_1}{0.0254s^2 + s + 1.53\beta_2} u_c \tag{4.7}$$

$$e = \frac{1.53\beta_1}{0.0254s^2 + s + 1.53\beta_2} u_c - G_m u_c \tag{4.8}$$

$$\frac{\partial e}{\partial \beta_1} = \frac{1.53 u_c}{0.0254s^2 + s + 1.53\beta_2} \tag{4.9}$$

$$\frac{\partial e}{\partial \beta_2} = -\frac{1.53}{0.0254s^2 + s + 1.53\beta_2} y_{plant} \tag{4.10}$$

The sensitivity derivatives obtained contains the parameter from the plant; however, the premise of the design with MRAC assumes that the plant characteristics are not absolutely known. The goal is to make the plant approach the model, if the model is close to the actual plant, the model characteristics can be substituted for the plants characteristics, giving the following sensitivity derivatives:

$$\tau s^2 + s + 1.53\theta_2 \cong s^2 + a_{1m}s + a_{0m} \tag{4.11}$$

$$\frac{\partial e}{\partial \beta_1} = \frac{a_{1m}s + a_{0m}}{s^2 + a_{1m}s + a_{0m}} u_c \tag{4.12}$$

$$\frac{\partial e}{\partial \beta_2} = -\frac{a_{1m}s + a_{0m}}{s^2 + a_{1m}s + a_{0m}} y_{plant} \tag{4.13}$$

With these approximations we get the following equations for updating the controller parameters:

$$\frac{d\beta_1}{dt} = -\gamma \frac{\partial e}{\partial \beta_1} e = -\gamma \left(\frac{a_{1m}s + a_{0m}}{s^2 + a_{1m}s + a_{0m}} u_c\right) e \tag{4.14}$$

$$\frac{d\beta_2}{dt} = -\gamma \frac{\partial e}{\partial \beta_2} = \gamma \left(\frac{a_{1m}s + a_{0m}}{s^2 + a_{1m}s + a_{0m}} y_{plant}\right) e \tag{4.15}$$

4.1 Tracking and synchronization control goal

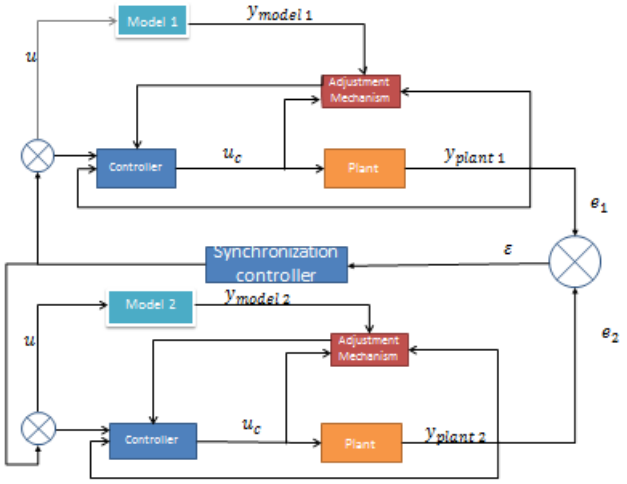

Figure 3: Block diagram of multi-agent setup

Let $S(\rho, t)$ be a time varying desired shape in a compact set, where ρ denote a state vector and t the time. The boundary of $S(\rho, t)$ is parameterized by a curve, denoted by $\partial S(\rho, t) = 0$

$x_i(t)$ *and* $x_i^d(t)$ are generalized state coordinates and its desired value of the ith agent, respectively, where $i = 1, \dots, n$, is an index.$x_i^d(t)$ locates on the desired curve such that $\partial S(x_i^d, t) = 0$. The state error of the ith agent is represented as;

$$e_i(t) = x_i^d(t) - x_i(t) \tag{4.16}$$

The control objective is converging each agent to its desired state $x_i^d(t)$ such that $e_i \to 0 \; as \; t \to \infty$.

The constraints may be expressed as follows;

$$\partial S(x_i, t) = 0 \tag{4.17}$$
$$x_i, (t) = A_i(t)C(t) + B_i(t)$$

Where $A_i(t)$ is a constraint matrix formulated based on the desired boundary, which depends on the characteristics of the ith agent; $C(t)$ is a common vector applicable to all agents and not on individual agents; $B_i(t)$ is an offset of the ith agent.

All the agents are linked via a common vector C(t), which requires a linear mapping from $x_i(t)$ to the common vector C(t) denoted by $\{x_i(t) \mapsto C(t)\}$. Therefore inverse of the constraint matrix $A_i(t)$ must exist.

The following assumptions are given:

Assumption 1.1: The desired boundary $\partial S(x_i, t) = 0$ is properly designed such that the inverse of the constraint matrix $A_i(t)$ exist.

From assumption 1.1 and Equation (3.2), it follows

That;

$$A_i^{-1}(t)\big(x_i(t) - B_i(t)\big) = C(t) \tag{4.18}$$

$$A_1^{-1}(t)\big(x_1(t) - B_1(t)\big) = A_2^{-1}(t)\big(x_2(t) - B_2(t)\big) = \cdots = A_n^{-1}(t)\big(x_n(t) - B_n(t)\big) = C(t) \tag{4.19}$$

The constraint equation must be valid to the desired coordinates $x_i^d(t)$, that is;

$$A_1^{-1}(t)\left(x_1^d(t) - B_1(t)\right) = A_2^{-1}(t)\left(x_2^d(t) - B_2(t)\right) = \cdots = A_n^{-1}(t)\big(x_n^d(t) - B_n(t)\big) = C(t) \tag{4.20}$$

Subtracting (4.1.5) from (4.1.4) utilizing (4.1.1) yield

$$A_1^{-1}(t)e_1(t) = A_2^{-1}(t)e_2(t) = \cdots = A_n^{-1}(t)e_n(t) \tag{4.21}$$

Let $c_i(t) \equiv A_i^{-1}(t)$ as the coupling parameter of the ith agent. Then (3.6) is,

$$c_1(t)e_1(t) = c_2(t)e_2(t) = \cdots = c_n(t)e_n(t) \tag{4.22}$$

$$\varepsilon_1 = c_1(t)e_1(t) - c_2(t)e_2(t) \tag{4.23}$$

Equation (4.1.7) represents a relationship that all position errors must be regulated to satisfy in order to ensure that the multiple agents meet the synchronization goal. From the final value theorem, the DC gain is given by;

$$DC\ gain = \lim_{t\to\infty} f(t) = \lim_{s\to 0} sF(s)\frac{\varepsilon}{s} = \lim_{s\to 0} F(s)\varepsilon = 0 \tag{4.24}$$

4.2 THREE AGENTS SYNCHRONIZATION LAYOUT

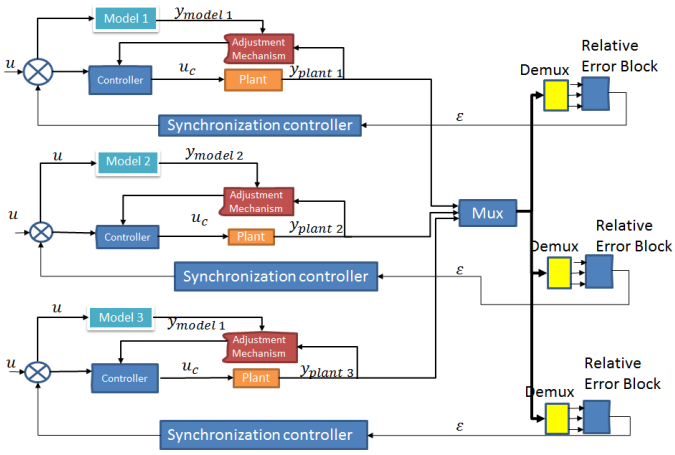

Figure 4: Layout of 3-Agents multi-axis synchronization

Synchronization of the three agents is achieved in the adaptive synchronization by employing the Relative Coupling Strategy. In this technique, each agent has its own relative error block, error from each of the agents is subtracted for the other agents. The error signal coming to the relative error block from the agent under analysis is considered positive and all other agents are considered negative. For example, the error from agent 1 of the adaptive synchronization coming to the relative error block 1 is give a positive sign and errors of agents 2 and 3 are given negative signs and subtracted individually from agent 1. The final relative differences are added and taken through the synchronization controller and the output from the synchronization controller is fed back. This ensures an effective synchronization.

5.0 SIMULATION AND EXPERIMENT

Two reference models are considered, namely;

- Critically damped reference model with roots
- $s = -20, -20;\ \zeta = 1;\ \omega_n = 20$
- Over-damped reference model roots
- $s = -45 \pm 33.54i;\ \zeta = 1.5,\ \omega_n = 30$

The reference models are chosen such that the over-damped reference model has more stable roots. For each reference model, tests are conducted in 3 different modes;

a. Without synchronization controller
b. With a critically damped synchronization controller
c. With an over-damped synchronization controller.

To investigate the adaptive synchronization performance; one of the agents is eccentrically loaded with a 100g weight, 10cm off center. The plot shows very good tracking properties even under the inertia disturbance. This is possible because the sensitivity derivative is able to adjust the parameter such that the error approaches zero.

Simulation results was obtained by applying the proposed control scheme to a mathematical model in Simulink as shown for various scenarios of over-damped and critically-damped reference Models with and without a synchronization controller. To emulate actual synchronization of the two agents with a load torque disturbance in simulation, a 50% load is applied to one of the agents representing a change in inertia through a slider gain block.

Figures 5 and 6 show simulation and experimental results respectively of synchronization error outputs for the critically-damped and over-damped reference models for two agents plotted on the same axis. The top row of each figure represents the case without the synchronization controller, middle row with a critically-damped synchronization controller, and bottom row with an over-damped synchronization controller. The synchronization error plots of figures 5 and 6 show transient and steady-state errors for the critically-damped and over-damped reference models of each.

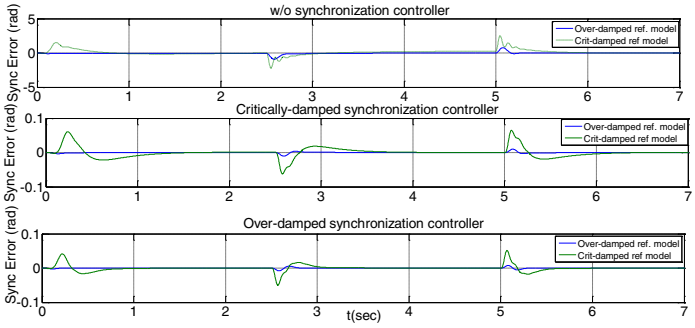

Figure 5: Superimposed simulated synchronization error plot: over-damped and critically-damped reference model

	Critically-damped Ref. Model (Transient sync. error/rad)	Over-damped Ref. Model (Transient sync. error/rad)
Without sync. controller	2.6	0.8
With critically-damp sync. controller	0.065	0.01
With over-damp sync. controller and more stable root	0.05	0.01

Table 1: Synchronization error results summary from simulation

Simulation results from Fig.5 show in all cases with or without a synchronization controller a steady-state error of 0rad. Results show with a critically-damp reference model, 97.7% and 98% reduction in transient error using a critically-damp synchronization controller and an over-damp synchronization controller respectively. With an over-damp reference model, both the critically-damp and the over-damp synchronization controllers equally show 98.8% reduction in transient error compared to the scenario without a synchronization controller.

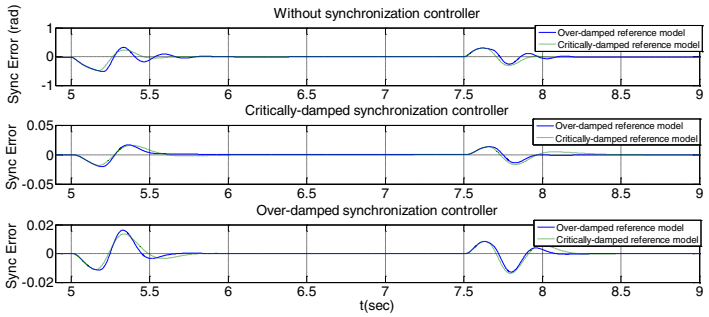

Figure 6: Superimposed experimental synchronization error plot; over-damped and critically damped reference model

	Critically-damp Ref. Model (Transient sync. error/rad)	Over-damp Ref. Model (Transient sync. error/rad)
Without sync. controller	0.4	0.42
With critically-damp sync. controller	0.018	0.018
With over-damp sync. controller and more stable root	0.012	0.012

Table 2: Synchronization error results summary from experiment

Experimental results from Fig. 6 show initial transient oscillations and steady-state error of zero without the synchronization controller. With the synchronization controller, a reduction in transient error of 95.5% and 97% using a critically-damp and an over-damp synchronization controller respectively are realized. In general, a faster settling time is seen with an over-damped reference model.

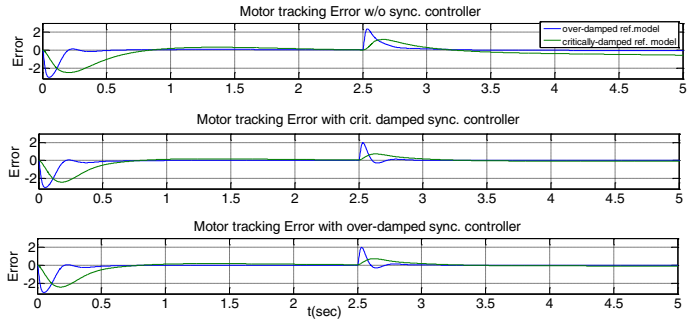

Figure 7: Superimposed simulated tracking error: over-damped and critically damped reference model

	Critically-damp Ref. Model (Transient tracking error/rad)	Over-damp Ref. Model (Transient tracking error/rad)
Without sync. controller	1.5	2.4
With critically-damp sync. controller	0.7	2.0
With over-damp sync. controller and more stable root	0.7	2.0

Table 3: Simulated tracking error performance

Figure 7 shows simulated tracking error output obtained from a comparison of the reference model output to the plant's output. There is a significant level of improvement in tracking performance with the use of a synchronization controller from simulation. A sluggish performance is seen without the synchronization controller. The critically-damp reference model indicated 53.3% reduction in transient tracking error with both critically-damp and over-damp synchronization controllers. The over-damp reference model resulted in 16.6% reduction in transient tracking error for both over-damped and critically-damp synchronization controllers. Additionally, the over-damp reference model shows approximately 0.4seconds reduction in settling time.

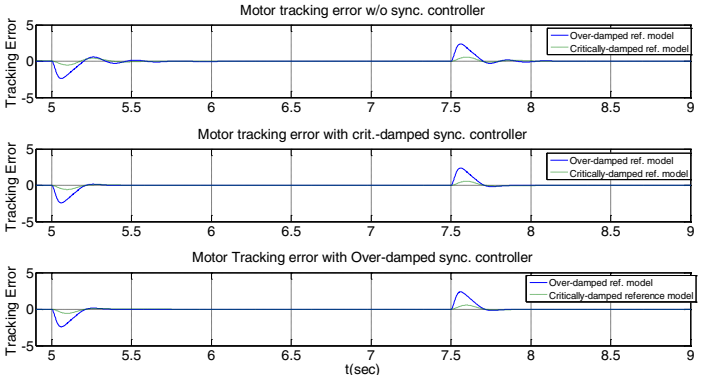

Figure 8: Superimposed experimental tracking error plot; critically-damped and over-damped reference model

	Critically-damp Ref. Model (Transient tracking error/rad)	Over-damp Ref. Model (Transient tracking error/rad)
Without sync. controller	0.4	2.2
Critically-damp sync. controller	0.4	2.2
Over-damp sync. controller and more stable root	0.4	2.2

Table 4: Experimental tracking error performance

In Figure 8, the tracking error plots from actual experiment are shown. No observable difference is seen in tracking error with use of a synchronization controller from actual experiment. However, oscillations are seen without the use of a synchronization controller. For the critically damped reference model, maximum transient tracking error of 0.4rad and steady-state error of 0rad is observed in all cases with or without a synchronization controller. Over-damped reference model shows maximum transient error is 2.2rad with a steady-state error of 0rad. It can generally be observed that an over-damped reference model results in higher transient tracking error. This is due to the fact that with the higher frequency in the over-damped reference model, overshoot in transient response also increases.

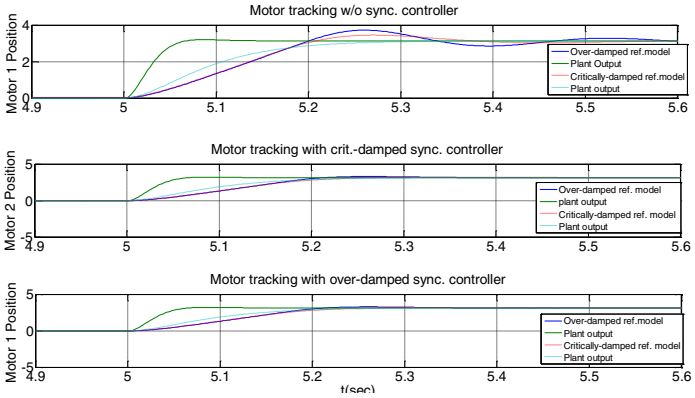

Figure 9: Tracking output: over-damped and critically damped reference model

Figure 9 shows tracking performance for over-damped reference model and plant response in bold outline, and that of critically-damped reference model and plant response in dashed outline. Similar performance in the plant's output is seen in both over-damped and critically-damped reference model. The use of a synchronization controller eliminates the oscillations and ensures a shorter settling time. The higher transient error observed in the tracking error plots with the use of an over-damped reference model can be seen. The synchronization controller is key in ensuring efficient and effective synchronization control. Similar performance tracking output from the plant is seen with both more stable roots and less stable roots reference models. Limitations in the actuator also contributes to the track error

The following results were obtained from synchronization of three agents;

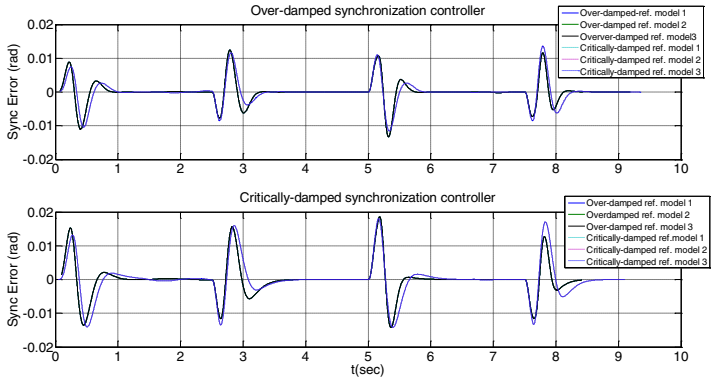

Figure 10: Superimposes synchronization error plot of three agents for over-damped and critically damper reference models

Similar synchronization error results to that obtained from the two agents is seen from the three agent synchronization in figure 10. This corroborates the proposed technique. Here again, a shorter settling time is observed with the use of an over-damped reference model.

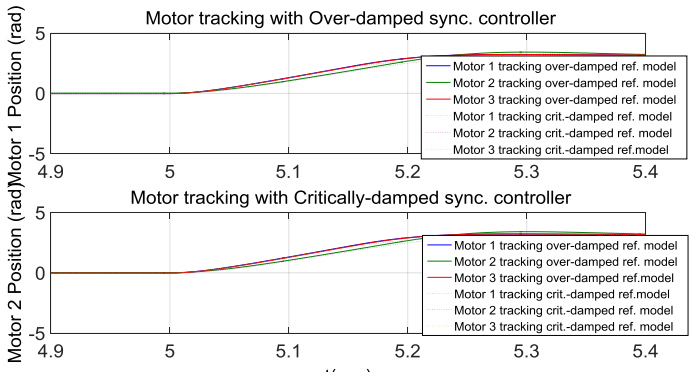

Figure 11: Three agents tracking output for over-damped and critically damped reference models

Figure 11 shows the tracking performance output for the three agent synchronization model. Precise synchronization and tracking is obtained from the architecture elaborating how n-agents could be synchronized.

CONCLUSION

An adaptive synchronization of networked multi-agent systems was investigated. Results from modeling, analysis, simulation and experiment were presented. A further experiment done with three agents was also presented to illustrate the application of the architecture to n-agents. The developed controller was implemented on networked DC servo-motor systems for validation. The approach improves synchronization properties in the multi-agent system compared to existing methods.

An improvement in disturbance rejection properties of approximately 95-97% in the transient errors was shown through the synchronization error plots. The simulations and experiments demonstrate the adaptive control system with the synchronization controller offers high dynamic stiffness against load disturbance.

Future works will look at synchronization control via Internet using UDP and remote hosts, and implementation of synchronization control at higher frequency adaptation.

ACKNOWLEDGEMENT

This material is based on research sponsored by Air Force Research Laboratory and OSD under agreement number FA8750-15-2-0116. The U.S. Government is authorized to reproduce and distribute reprints for Governmental purposes notwithstanding any copyright notation thereon.

REFERENCES

1. Perez-Pinal, F.J., et al. Comparison of multi-motor synchronization techniques. 30th Annual Conference of Industrial Electronics Society, 2004. IECON 2004. **2**: p. 1670-1675
2. Rapini, D., New Directions In Motion Control. Motion Control, 1999: p. 37-38.
3. Anderson, R.G., et al., Web machine coordinated motion control via electronic line-shafting. IEEE Transactions on Industry Applications, 2001. **37**(1): p. 247-254.
4. Valenzuela, M.A. and R.D. Lorenz, Electronic line-shafting control for paper machine drives. IEEE Transactions on Industry Applications, 2001. **37**(1): p. 158-164.
5. Tomizuka, M., et al., Synchronization of two motion control axes under adaptive feedforward control. Journal of dynamic systems, measurement, and control, 1992. **114**(2): p. 196-203.
6. Uchiyama, M. and Y. Nakamura. Symmetric hybrid position/force control of two cooperating robot manipulators. IEEE International Workshop on Intelligent Robots. 1988: p. 515-520.
7. Perez-Pinal, F.J., et al. Comparison of multi-motor synchronization techniques. 30th Annual Conference of Industrial Electronics Society, 2004. IECON 2004. **2**: p. 1670-1675.
8. Ishizaki, K., B. Sencer, and E. Shamoto, Cross Coupling Controller for Accurate Motion Synchronization of Dual Servo Systems. Journal ref: International Journal of Automation Technology, 2013. **7**(5): p. 514-522.
9. Cheng, M.H., C.-Y. Chen, and E.G. Bakhoum, Synchronization controller synthesis of multi-axis motion system.
10. Cheng, M.H.-M., A. Mitra, and C.-Y. Chen. Synchronization controller synthesis of multi-axis motion system. IEEE Fourth International Conference on Innovative Computing, Information and Control (ICICIC), 2009.
11. Sun, D., Synchronization and control of multiagent systems. Vol. 41. 2010: CRC Press.
12. Sun, D., Position synchronization of multiple motion axes with adaptive coupling control. Automatica, 2003. **39**(6): p. 997-1005.
13. Sun, D., et al., A synchronization approach to trajectory tracking of multiple mobile robots while maintaining time-varying formations IEEE Transactions on Robotics, 2009. **25**(5): p. 1074-1086.
14. Ehsani, M.S. Adaptive Control of Servo Motor by MRAC Method. IEEEC onference on Vehicle Power and Propulsion, 2007. VPPC
15. Benjelloun, K., H. Mechlih, and E.K. Boukas. A modified model reference adaptive control algorithm for DC servomotor. Second IEEE Conference on Control Applications, 1993.
16. Swarnkar, P., S. Jain, and R. Nema, Effect of adaptation gain on system performance for model reference adaptive control scheme using MIT rule. World Academy of science, engineering and technology, 2010. **70**: p. 621-626.